











ULF geomagnetic anomaly associated with the Sumatra-Pagai Islands earthquake swarm during 2020

Marzuki MARZUKI^{1,*} , Muhammad HAMIDI¹ , Suaidi AHADI² ,
Ardian PUTRA¹ , Afdal AFDAL¹ , Harmadi HARMADI¹ ,
Dwikorita KARNAWATI² , Hendra Suwarta SUPRIHATIN² ,
Muhammad SYIROJUDIN² , Indah MARSYAM² 

¹ Departement of Physics, Universitas Andalas, Padang 25163, Indonesia;
e-mails: marzuki@sci.unand.ac.id, hamidhy1208@gmail.com, ardianputra@sci.unand.ac.id,
afdal@sci.unand.ac.id, harmadi@sci.unand.ac.id

² Meteorology Climatology and Geophysical Agency, Jakarta 10720, Indonesia;
e-mails: suaidi.ahadi@bmkg.go.id, dwikorita@bmkg.go.id, hendrasuwarta60@gmail.com,
syirojudin.bmkg@gmail.com, indahmarsyam.vc@gmail.com

Abstract: Observations of earthquake precursors via geomagnetic anomalies from ultra-low frequency (ULF) could provide an expectation for short-term earthquake prediction. However, there are still several obstacles in determining this precursor, one of which is the presence of a precursor bias if the earthquake occurs at a close time and location. To cope with this problem, we analysed six earthquakes with a magnitude > 5 on Pagai Island, Mentawai, Sumatra, during 2020. These earthquakes have epicentres close to each other and occur within a short time (one month). This study used geomagnetic data recorded by the Magnetic Data Acquisition System (MAGDAS) magnetometer network at Sicincin station (SCN), West Sumatra, and Kepahiyang station (KPY), Bengkulu, with a span of one month before the earthquake. The anomaly of ULF emission was analysed using the power spectral density method at a frequency of 0.012 Hz for the H and Z components of the geomagnetic data. The onset time of the ULF emission anomaly was determined by the standard deviation value ($pz + \sigma$, $pz - \sigma$) of the S_Z/S_H power ratio polarization. The disturbance storm time index (Dst) was used to ensure that the anomaly occurred was not caused by geomagnetic storm. Also, the single station transfer function was used to calculate the azimuth, and the empirical formula between the anomaly amplitude and the magnitude was used to calculate the earthquake magnitude as the validation of the anomaly source. Several ULF anomalies as earthquake precursors were observed, especially at the KPY station. The estimated azimuth shows a good accuracy compared to the earthquake's azimuth, with an average value of 97.8%. Furthermore, the earthquake magnitude calculated from the ULF anomaly shows a good agreement with the actual earthquake magnitude, with an average accuracy of 98.13%. Thus, the azimuth and mag-

*corresponding author, e-mail: marzuki@sci.unand.ac.id

nitide estimation technique effectively determined precursors for earthquakes with the adjacent time of occurrence and source locations. However, it is recommended to observe precursors using several stations because the precursors are sometimes not observed by one station but observed by others.

Key words: ultra low frequency, earthquake precursor, MAGDAS, Pagai Islands, Sumatra

1. Introduction

Short-term earthquake prediction is critical in improving the preparation in facing the earthquake disaster. One method considered very promising for short-term earthquake prediction is by observing ultra-low frequency (ULF) anomaly before, during and after the earthquake (*Hattori et al., 2002a; 2002b*). The study of ULF emission anomaly as an earthquake precursor was conducted by observing the emission of electromagnetic waves at a frequency < 0.1 Hz based on geomagnetic data from ground observatories. The study was conducted to monitor seismogenic activity before, during and after an earthquake through the observation of a magnetometer on the earth's surface. Seismogenic activity prior to an earthquake can produce some changes in electric properties of the lithosphere. This process emits electromagnetic waves from the ultra-low frequency (ULF) to very high frequency (VHF) bands, but only ULF is detected by the magnetometer on the earth's surface for being slightly attenuated. Related to earthquakes, there are three mechanisms for generating ULF emissions, i.e. micro-fracturing effect, electrokinetic effect, and induction effect. The micro-fracturing effect is in the form of a ULF emission model related to the main earthquake (mainshock) where, if a rock fracture occurs, the emission of electromagnetic waves in the recorded ULF spectrum will significantly increase at the earthquake source (*Molchanov and Hayakawa, 1995*). *Molchanov and Hayakawa (1998)* proposed micro-fracturing as one of the possibilities in searching for the electromagnetic emission mechanism in the ULF frequency band. Electrokinetic effects in the form of pressure changes in rock fractures that produce electrokinetic flows caused by silica deposits in these rocks produce the geomagnetic disturbance flows. The electrokinetic effect occurred before the Loma Prieta earthquake in 1989 where the electrokinetic effect resulted in a mass flow of electron particles caused by rock fractures that were pro-

portional to the magnitude and frequency of the geomagnetic disturbance signal. The induction effect in the form of changes in geo-electrical conductivity in the lithosphere due to activity in the focal zone causes the changes in the amplitude of non-lithospheric electromagnetic waves (Mogi, 1985).

ULF emission can be calculated from geomagnetic data using the power spectral density (PSD) method and wavelet method. The results of the calculation are then analysed for the polarization value of the power ratio of the vertical component (S_Z) and the horizontal component (S_H) of the geomagnetic signal (Ahadi et al., 2015; Saroso et al., 2009; Yumoto et al., 2009). ULF emission anomaly is determined from the polarization value of the power ratio of S_Z and S_H , which exceeds the standard deviation value (Ahadi et al., 2015). The disturbance storm index (Dst) is used as validation to ensure that the anomaly source is not external disturbances such as geomagnetic activity. The impact of external disturbances such as geomagnetic storms will more significantly affect the intensity of the horizontal component of the geomagnetic signal (H) rather than the vertical component (Z) (Ahadi et al., 2014). The Dst index is also used to observe geomagnetic activity recorded in the equatorial and low latitude areas (Saroso et al., 2009). In addition, to ascertain if the ULF emission anomaly occurred is caused by seismogenic activity, the single station transfer function (SSTF) method is used to ensure the direction of the anomaly source known as azimuth. ULF emission anomaly indicated as precursors refer to the anomaly that points to the earthquake source.

Though there have been many studies on geomagnetic precursors related to the earthquake, some points become the drawbacks in searching for this precursor, such as the existence of precursor bias if the earthquake occurs in the adjacent time and location. Therefore, this study analyses earthquake events that occurred in Pagai Island, Mentawai, Sumatra, with the adjacent time and location. Six earthquakes with a magnitude > 5 Mw in Pagai Island, during October–November 2020 were analysed. Pagai Island has active seismotectonic activity because it is located in the plate subduction zone and the Mentawai megathrust zone. Historically, the epicentres of earthquakes in Pagai Island are close to each other. The research on geomagnetic precursor related the earthquake occurred in Pagai Island, Mentawai had been conducted by Ibrahim et al. (2012). They observed the presence of ULF anomaly observed in Kototabang (KTB) station, Agam Regency, for

5 days before the earthquake. *Ahadi et al. (2015)* conducted other research showing the anomaly of ULF emission as the precursor several days before the occurrence of earthquake in Pagai Island as detected from KTB station with the onset time of ULF emission anomaly within 3 to 11 days before the earthquake. Also, *Purba et al. (2013)* observed the ULF anomaly as the precursor occurred from 17 to 21 days before the Mentawai earthquake as detected by KTB station. The studies above were conducted using the data of the main earthquake (mainshock) with a magnitude > 6 . From several studies related to the precursor in Pagai Island, no studies performed the analysis for the earthquake occurred in the adjacent time and location. This research aimed to see the effectiveness of the ULF emission anomaly precursor related to such an earthquake. Also, the results of this research could support previous studies related to ULF emission as the precursor of earthquakes in particular in Pagai and in general in Sumatra.

2. Data and method

2.1. Instrument and data

This study analysed six earthquakes data in Pagai Island, Mentawai with a magnitude of > 5 , at a depth of ≤ 60 km and at a distance of ≤ 500 km from the observation station. The distribution and list of earthquakes can be seen in Fig. 1 and Table 1. *Ahadi et al. (2014)* stated that ULF anomalies related to earthquakes with a magnitude of > 5 can still be detected at observation station with a distance of ≤ 500 km from the earthquake source. Of six earthquakes studied, five earthquakes were foreshock earthquakes with a thrust fault mechanism caused by plate subduction in the megathrust zone, Mentawai-Pagai, while the earthquake on November 17, 2020 ($M_W = 5.9$) was a shallow earthquake due to the fault activity in investigated fracture zone around the plate collision boundary, which has a strike-slip fault movement mechanism.

Earthquake data consists of several parameters: origin time, magnitude (M), depth of the hypocentre (h), distance of the hypocentre (d), and the azimuth angle of the earthquake source to the nearest station (θ_{EQ}), as seen in Table 1. Earthquake data were taken from Meteorology Climatology and Geophysical Agency (BMKG) catalogue (<http://repogempa.bmkg.go.id>),

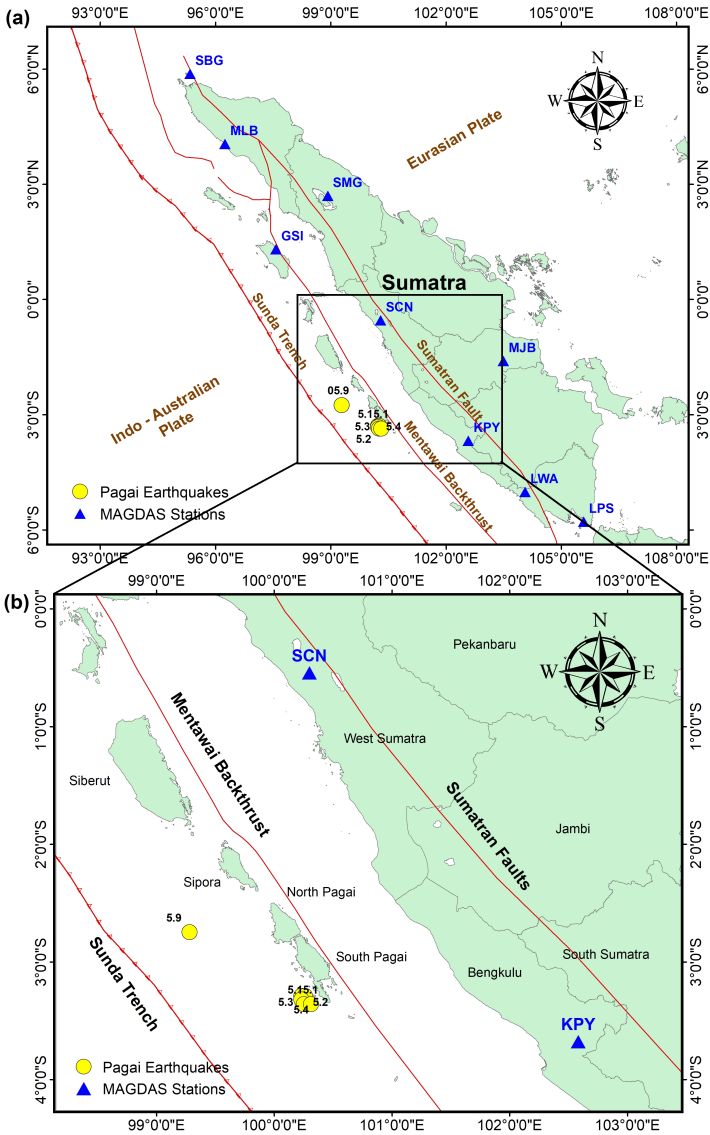


Fig. 1. (a) Locations of MAGDAS station in Sumatra (blue triangle), and earthquake cases analysed in this study (yellow circle). All earthquakes occurred during 2020. The map in panel (b) is an enlargement of the square area in panel (a). SCN and KPY indicate MAGDAS station at Sicincin (West Sumatra province) and Kepahiyang (Bengkulu province), respectively.

Table 1. Earthquake cases analysed in this study and their parameters.

No.	Date of EQ ¹	Time ² [LT]	Location ³		M_{EQ} ⁴ [M _W]	h ⁵ [km]	Sta ⁶ [code]	d ⁷ [km]	θ_{EQ} ⁸ [°]	K_S ⁹
			Lat [°N]	Lon [°E]						
1	October 15, 2020	16:41:16	−3.29	100.23	5.4	49	SCN	304	178	2.36
							KPY	265	286	2.56
2	October 17, 2020	07:26:02	−3.29	100.26	5.2	10	SCN	303	179	2.76
							KPY	262	282	3.04
3	October 18, 2020	00:55:00	−3.32	100.23	5.3	44	SCN	307	178	2.34
							KPY	264	277	2.56
4	October 19, 2020	05:48:50	−3.36	100.25	5.1	26	SCN	311	179	2.03
							KPY	262	276	2.22
5	October 21, 2020	21:35:09	−3.36	100.31	5.1	26	SCN	311	180	2.03
							KPY	255	278	2.25
6	November 17, 2020	08:44:07	−2.75	99.28	5.9	10	SCN	267	160	20.30
							KPY	381	279	14.53

¹ Date of earthquake, ² time of occurrence in local time (LT), ³ location of earthquake source, ⁴ earthquake magnitude, ⁵ depth of earthquake hypocentre, ⁶ observation station closest to the earthquake source (station code), ⁷ distance of earthquake to observation station, ⁸ azimuth of earthquake to observation station, ⁹ earthquake local seismic index.

with a magnitude in the form of moment magnitude (M_W), hence, it must be converted to surface magnitude (M_S) to calculate the value of the seismic index (K_S). This index represents the impact of the earthquake on the nearest observation station (*Scordilis, 2006*). The conversion of moment magnitude (M_W) to surface magnitude (M_S) used the following formula:

$$M_W = 0.67 (\pm 0.005) M_S + 2.07 \quad \text{for } 3.0 \leq M_S \leq 6.2, \tag{1}$$

$$M_W = 0.99 (\pm 0.020) M_S + 0.08 \quad \text{for } 6.2 < M_S \leq 8.2. \tag{2}$$

Seismic index (K_S) was calculated by *Molchanov et al. (2003)*:

$$K_S = \left(1 + R^{\frac{-M_S}{2}} \right)^{-2.33} + \frac{10^{0.75M_S}}{10R}, \tag{3}$$

where M_S refers to the surface magnitude, and R is the distance from the earthquake source to the observation station.

The geomagnetic data used were H and Z component of geomagnetic field data that has a sampling rate 1 second with a time span of one month before the earthquake. The data were recorded by MAGDAS magnetometer at Climatology Station Class II, Sicincin (SCN), Padang Pariaman, West Sumatra (-0.54° N, 100.29° E) and Geophysics Station Class III Kepahiang (KPY), Bengkulu (-3.67° N, 102.58° E). The MAGDAS stations are operated by BMKG. The location of the MAGDAS station can be seen in Fig. 1. Table 2 presents the specifications of the MAGDAS magnetometer used in this study.

Table 2. Specification of MAGDAS magnetometer.

Location of station	Sicincin, West Sumatra	Kepahiyang, Bengkulu
Station code	SCN	KPY
Type of sensor	MAGDAS-9	MAGDAS-9
Measurement component	H, D, Z	H, D, Z
Sampling rate	1 Hz	1 Hz

To ascertain that the ULF anomaly occurred was not the result of external disturbances such as geomagnetic activity, we used Dst index (*Uozumi et al., 2008*). This index can be accessed through <http://wdc.kugi.kyoto-u.ac.jp> owned by WDC Geomagnetic Models, Kyoto University. Table 3 presents the classification of solar storms based on the Dst index.

Table 3. Classification of solar storms based on the Dst index.

No.	Storm Category	Index Range (nT)
1	Weak	$-30 \geq \text{Dst} > -50$
2	Moderate	$-50 \geq \text{Dst} > -100$
3	Strong	$-100 \geq \text{Dst} > -200$
4	Very Strong	$-200 \geq \text{Dst} > -300$
5	Super	$\text{Dst} \leq -300$

2.2. Identification of ULF emission anomaly

The ULF emission anomaly was identified by analysing the geomagnetic signal in the frequency domain with the sampling rate (ν) of the instrument used, as given by:

$$f_{Nyquist} = \frac{1}{2} v. \quad (4)$$

This study uses an instrument with a sampling rate of 1 Hz, so the maximum frequency is 0.5 Hz, as in *Yumoto et al. (2009)*. The calculation used the power spectral density (PSD) with the Welch method, which divided the signal into N data in several segments, which were overlapped by 50% for each segment. In each segment, Fast Fourier Transform (FFT) called as nFFT was carried out with Window Hamming type with a width of $L = N + 1$ using the following formula:

$$E(P_{Welch}) = \frac{1}{f_s L_s} \int_{-f_s}^{f_s} P_{xx}(p) |W(f - p)|^2 dp, \quad (5)$$

where f_s is the sampling frequency, L_s is the data length in one segment, U is the normalization of the periodogram (P_{xx}), W is the rectangular window used in signal processing, i.e. 1024, and f is the selected frequency. The frequency spectrum chosen in this study was 0.012 Hz, on which earthquake-related anomaly was clearly visible (*Han et al., 2011; Hattori et al., 2011; Hattori et al., 2013; Molchanov et al., 2003*). The results of the PSD showed the values of the Z and H components. Then, the daily S_Z/S_H power ratio polarization technique was carried out for each observation station using the following equation (*Prattes et al., 2011*):

$$P_{day} = \frac{Z_{day}}{H_{day}}, \quad (6)$$

where P_{day} is power ratio polarization of Z and H component and Z_{day} refers to the daily values of Z component and H_{day} is the daily value of H component, given by (*Prattes et al., 2011*):

$$Z_{day} = \frac{S \sum Z_{day} - \mu \sum Z_{month}}{\sigma \sum Z_{month}}, \quad (7)$$

$$H_{day} = \frac{S \sum H_{day} - \mu \sum H_{month}}{\sigma \sum H_{month}}. \quad (8)$$

The control towards the standard deviation of the results of the S_Z/S_H power ratio polarization was carried out then. The S_Z/S_H values exceeding the moving average value from the standard deviation limit ($pz + \sigma, pz - \sigma$) was expressed as the onset time of the ULF emission anomaly.

2.3. Estimation of earthquake source location

Geomagnetic anomaly induction direction was determined using the Single Station Transfer Function (SSTF) method (*Hattori, 2004*). This method aims to determine the direction of disturbance caused by ULF emission from the earth's lithosphere. The linear relationship between the three components of the Earth's magnetic field is:

$$\Delta Z(\omega) = A(\omega) \cdot \Delta X(\omega) + B(\omega) \cdot \Delta Y(\omega), \quad (9)$$

where $\Delta Z(\omega)$ is the north–south geographic component of earth, $Y(\omega)$ is the geographical east–west component of the earth, $\Delta X(\omega)$ is the vertical component of the earth's magnet as a mathematical component of the Fourier complex (*Rikitake and Honkura, 1985*). The coefficients $A(\omega)$ and $B(\omega)$ are considered as the invariants and as the complex transfer functions in the frequency domain. The transfer function has information about the electrical conductivity under the ground surface, which is called as Conductivity Anomaly (CA). In addition, the transfer function also has information about the direction of the induction (Parkinson vector) whose length and direction indicate the magnitude and direction of the source of the magnetic anomaly, expressed by (*Parkinson, 1959*):

$$Amp(\omega) = \sqrt{A_{Re}^2(\omega) + B_{Re}^2(\omega)}, \quad (10)$$

$$\theta(\omega) = \tan^{-1} \left[\frac{A_{Re}(\omega)}{B_{Re}(\omega)} \right], \quad (11)$$

where $Amp(\omega)$ is the conductivity (distance between the conductivity fields) and $\theta(\omega)$ is the direction of the anomaly source ($^{\circ}$) or called as the azimuth of anomaly. The earthquake source location was estimated from the ULF anomaly direction with an azimuth tolerance of 22.5° towards the top and bottom of the actual azimuth (*Armansyah et al., 2016*).

2.4. Earthquake magnitude estimation

The amplitude of the ULF emission anomaly was used to estimate the magnitude and position of the earthquake source to occur. This estimation was carried out based on the following empirical formulation as recommended by *BMKG (2019)*:

$$M = (0.0246 \times A) + 5.0948 \quad \text{for earthquakes in Subduction Zone,} \quad (12)$$

$$M = (0.0475 \times A) + 4.5983 \quad \text{for earthquakes in Sumatra Fault,} \quad (13)$$

where M is earthquake magnitude to occur and A refers to the anomaly amplitude of S_Z/S_H .

3. Results and discussion

3.1. ULF emission anomaly

Figure 2 shows the ULF emission anomaly during September–November 2020. The complete list of anomalies at SCN and KPY stations can be seen in Tables 4 and 5, respectively. Let us first discuss the anomaly before the earthquake of 15 October 2020 ($M_W = 5.4$). This was a foreshock earthquake occurred at a depth of 14 km in the southern area of Pagai (Fig. 1). This earthquake was 304 km from the SCN, Padang Pariaman with a magnitude of 5.4 M_W resulting in a seismic index of 2.36 and 258 km from KPY with a seismic index of 2.56 (Table 1). Polarization power ratio (S_Z/S_H) showed 6 ULF emission anomalies at the SCN station and 15 ULF emission anomalies at the KPY station, before 15 October 2020 earthquake ($M_W = 5.4$). The anomaly was indicated by polarization power ratio of the geomagnetic signal (blue line) passing the standard deviation (red line) (Fig. 2b and 2c). All of these anomalies in Fig. 2b and 2c cannot be considered as the precursors of the 15 October 15 2020 earthquake because a ULF anomaly as an earthquake precursor must meet certain conditions. An ULF anomaly can be considered as the earthquake precursors if (i) there is no influence of external factors such as geomagnetic activity, (ii) the azimuth generated by the anomaly leads to the earthquake source, and (iii) no two or more earthquakes occurred at the same time (*Ahadi, 2014*). The ascertainment of the external factors was carried out using the Dst index. There were several solar storm activities as indicated by a Dst index value of -30 nT to -57 nT, during 24–30 September, 2020 and October 5, 2020 (Fig. 2a). These geomagnetic activities were categorized as a weak to moderate storm (*Loewe and Prölss, 1997*), resulting in ULF emission anomaly on September 27 (08:00 LT) and October 29 (22:00 LT), indicated by black squares in Fig. 2. As the ULF anomalies during these times coincided with the anomaly due to geomagnetic activity; we did not consider it as an earth-

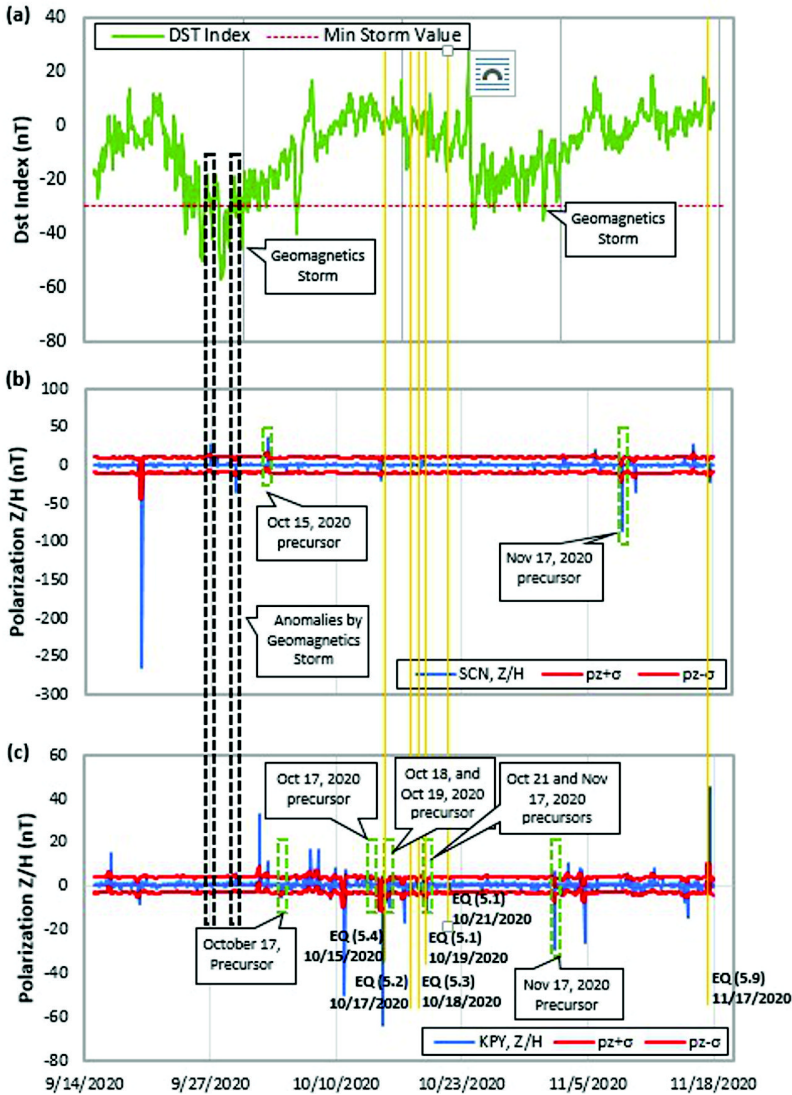


Fig. 2. (a) Dst Index (green line), (b) polarization of S_Z/S_H (blue line) at SCN station and (c) at KPY station, during September–November 2020. The Dst index below the horizontal line in Fig. 2a indicates a geomagnetic storm due to solar activity, including black rectangles. The red lines in Figs. 2b and 2c show $p_z + \sigma$ and $p_z - \sigma$ where σ is standard deviation of the power ratio polarization (p_z). The yellow vertical lines show the earthquake cases studied.

quake precursor. However, other anomalies did not coincide with the decline of Dst index so that the azimuth values of these anomalies were determined to ensure that the anomaly whether related to the earthquake or not.

In similar method, ULF anomalies that are candidates for precursors of other earthquake are also determined. Polarization power ratio for the earthquakes on October 17, 2020 ($M_W = 5.2$), October 18, 2020 ($M_W = 5.3$), October 19, 2020 ($M_W = 5.1$), October 21, 2020 ($M_W = 5.1$), and November 17, 2020 ($M_W = 5.9$) can be also seen in Fig. 2. Several declines in the value of the Dst index appeared before these earthquakes such as on

Table 4. ULF anomalies observed at SCN station.

No.	Date of An ¹	Time ² [LT]	θ_A ³ [°]	θ_{EQ} ⁴ [°]	$\Delta\theta$ ⁵ [°]	Date of An ⁶	Dst ⁷ [nT]	Not ⁸	Pre ⁹
1	September 20, 2020	06:00:00	71	178	107	October 15, 2020	-6	Azimuth not to EQ	No
2	September 27, 2020	08:00:00	-	-	-	-	-30	Geomagnetic storm	No
3	September 29, 2020	22:00:00	-	-	-	-	-34	Geomagnetic storm	No
4	October 3, 2020	06:00:00	165	178	13	October 15, 2020	-27	Azimuth and magnitudo estimation to EQ	Yes October 15, 2020 precursor
5	October 14, 2020	24:00:00	150	178	28	October 18, 2020	-1	Azimuth not to EQ	No
6	November 6, 2020	01:00:00	102	160	58	November 17, 2020	-18	Azimuth not to EQ	No
7	November 8, 2020	23:00:00	177	160	-17	November 17, 2020	-2	Azimuth and magnitudo estimation to EQ	Yes November 17, 2020 precursor
8	November 10, 2020	06:00:00	45	160	115	November 17, 2020	0	Azimuth not to EQ	No
9	November 16, 2020	08:00:00	74	160	68	November 17, 2020	9	Azimuth not to EQ	No

¹Date of ULF anomaly, ²time of anomaly occurrence, ³anomaly azimuth from SCN station, ⁴closest earthquake azimuth to the observation station, ⁵difference of anomaly azimuth to earthquake azimuth, ⁶closest earthquake to the observation station, ⁷Dst Index, ⁸the reason for being used as an earthquake precursor, ⁹the notes as an earthquake precursor.

Table 5. ULF anomalies observed at KPY station.

No.	Date of An ¹	Time ² [LT]	θ_A^3 [°]	θ_{EQ}^4 [°]	$\Delta\theta^5$ [°]	Date of An ⁶	Dst ⁷ [nT]	Not ⁸	Pre ⁹
1	September 17, 2020	01:00:00	109	282	173	October 17, 2020	-4	Azimuth not to EQ	No
2	September 19, 2020	24:00:00	170	276	106	October 19, 2020	-5	Azimuth not to EQ	No
3	September 29, 2020	24:00:00	-	-	-	-	-34	Geomagnetic storm	No
4	October 2, 2020	11:00:00	216	276	60	October 19, 2020	-22	Azimuth not to EQ	No
5	October 3, 2020	06:00:00	37	276	239	October 19, 2020	-27	Azimuth not to EQ	No
6	October 4, 2020	17:00:00	272	282	10	October 15, 2020	-1	Azimuth and magnitudo estimation to EQ	Yes October 17, 2020 precursor
7	October 7, 2020	06:00:00	141	276	135	October 19, 2020	2	Azimuth not to EQ	No
8	October 7, 2020	17:00:00	319	276	-43	October 19, 2020	14	Azimuth not to EQ	No
9	October 8, 2020	11:00:00	105	276	171	October 19, 2020	-6	Azimuth not to EQ	No
10	October 9, 2020	20:00:00	166	276	110	October 19, 2020	-1	Azimuth not to EQ	No
11	October 10, 2020	05:00:00	229	276	47	October 19, 2020	1	Azimuth not to EQ	No
12	October 11, 2020	05:00:00	167	276	109	October 19, 2020	0	Azimuth not to EQ	No
13	October 11, 2020	09:00:00	315	276	-39	October 19, 2020	7	Azimuth not to EQ	No
14	October 13, 2020	23:00:00	268	282	14	October 17, 2020	11	Azimuth and magnitudo estimation to EQ	Yes October 17, 2020 precursor
15	October 14, 2020	19:00:00	252	276	24	October 19, 2020	3	Azimuth not to EQ	No
16	October 15, 2020	03:00:00	292	277	15	October 18, 2020	-1	Azimuth and magnitudo estimation to EQ	Yes October 18, 2020 precursor

Table 5. Continued from the previous page.

No.	Date of An ¹	Time ² [LT]	θ_A^3 [°]	θ_{EQ}^4 [°]	$\Delta\theta^5$ [°]	Date of An ⁶	Dst ⁷ [nT]	Not ⁸	Pre ⁹
17	October 15, 2020	13:00:00	208	276	68	October 19, 2020	1	Azimuth not to EQ	No
18	October 15, 2020	20:00:00	266	276	10	October 19, 2020	1	Azimuth and magnitudo estimation to EQ	Yes October 19, 2020 precursor
19	October 17, 2020	08:00:00	281	282	1	October 19, 2020	-2	Azimuth and magnitudo estimation to EQ	Yes October 17, 2020 precursor
20	October 17, 2020	18:00:00	261	255	-6	October 21, 2020	-5	Azimuth and magnitudo estimation to EQ	Yes October 21, 2020 precursor
21	October 19, 2020	17:00:00	87	255	168	November 17, 2020	-9	Azimuth not to EQ	No
22	October 25, 2020	09:00:00	205	279	74	November 17, 2020	-11	Azimuth not to EQ	No
23	October 25, 2020	24:00:00	329	279	-50	November 17, 2020	-28	Azimuth not to EQ	No
24	October 31, 2020	05:00:00	154	279	125	November 17, 2020	-9	Azimuth not to EQ	No
25	November 1, 2020	21:00:00	53	279	226	November 17, 2020	-6	Azimuth not to EQ	No
26	November 1, 2020	23:00:00	284	279	-5	November 17, 2020	-17	Azimuth and magnitudo estimation to EQ	Yes November 17, 2020 precursor
27	November 3, 2020	06:00:00	167	279	112	November 17, 2020	-14	Azimuth not to EQ	No
28	November 4, 2020	13:00:00	325	279	-46	November 17, 2020	-6	Azimuth not to EQ	No
29	November 4, 2020	24:00:00	133	279	146	November 17, 2020	4	Azimuth not to EQ	No
30	November 9, 2020	11:00:00	120	279	159	November 17, 2020	-4	Azimuth not to EQ	No
31	November 9, 2020	20:00:00	148	279	131	November 17, 2020	-2	Azimuth not to EQ	No

Table 5. Continued from the previous page.

No.	Date of An ¹	Time ² [LT]	θ_A ³ [°]	θ_{EQ} ⁴ [°]	$\Delta\theta$ ⁵ [°]	Date of An ⁶	Dst ⁷ [nT]	Not ⁸	Pre ⁹
32	November 12, 2020	04:00:00	156	279	123	November 17, 2020	13	Azimuth not to EQ	No
33	November 15, 2020	07:00:00	201	279	78	November 17, 2020	0	Azimuth not to EQ	No
34	November 15, 2020	15:00:00	324	279	−45	November 17, 2020	4	Azimuth not to EQ	No

¹ Date of ULF anomaly, ² time of anomaly occurrence, ³ anomaly azimuth from KPY station, ⁴ closest earthquake azimuth to the observation station, ⁵ difference of anomaly azimuth to earthquake azimuth, ⁶ closest earthquake to the observation station, ⁷ Dst Index, ⁸ the reason for being used as an earthquake precursor, ⁹ the notes as an earthquake precursor.

September 24–30, October 5, and November 24–31, 2020. Thus, the ULF emission anomaly on September 27, 2020 and September 29, 2020 coincided with a solar storm; thus they cannot be considered as a candidate for earthquake precursors. Several ULF emission anomalies occurred on quiet days (no solar storm activity) such as anomalies on September 19, 2020 (21:00 LT), September 20, 2020 (06:00 LT) at SCN station and September 19, 2020 (24:00 LT), October 2, 2020 (11:00 LT) at KPY station, can be suspected as precursors for the earthquake in October 17, 2020 ($M_W = 5.2$), October 18, 2020 ($M_W = 5.3$), October 19, 2020 ($M_W = 5.1$), October 21, 2020 ($M_W = 5.1$), and November 17, 2020 ($M_W = 5.9$). Therefore, the azimuth values of these anomalies were evaluated to ensure that the anomaly was related to the earthquake, as discussed in the next section.

3.2. Estimation of earthquake source location

In this section, the azimuth value was calculated for the ULF emission anomaly which did not occur simultaneously with the anomaly due to geomagnetic activity. An ULF anomaly can be considered as the earthquake precursors if the azimuth generated by the anomaly leads to the earthquake source. Figure 3 showed the azimuth of ULF anomaly pointing to the earthquake source of 15 October 2020 ($M_W = 5.4$) (yellow circle), calculated from SCN station (blue triangle). The 15 October 2020 earthquake ($M_W = 5.4$) was a tectonic earthquake in view of the plate subduction in the megath-

rust zone of Mentawai-Pagai (-3.21° N, 100.31° E). Thus, the anomaly that can be assumed as a precursor to this earthquake based on the azimuth value was an anomaly that had an azimuth towards the megathrust zone of Mentawai-Pagai. Of the three anomalies at the SCN station before 15 October 2020 that did not coincide with the geomagnetic storm (Fig. 2 and Table 4), only the anomaly of 3 October 2020 (06:00 LT) had azimuths pointing to the earthquake source. The azimuth of this anomaly was 165° towards the SCN station to the south (red arrow in Fig. 3). With a tolerance azimuth of 22.5° (Armansyah et al., 2016), the estimated azimuth value of the ULF anomaly value was $187.5^\circ - 142.5^\circ$ (blue lines in Fig. 3, clockwise with the zero point in the north). The actual azimuth generated by the earthquake of October 15, 2020 ($M_W = 5.4$) was 178° to the SCN station and 282° to the KPY station (Table 4). Thus, the earthquake source was within the

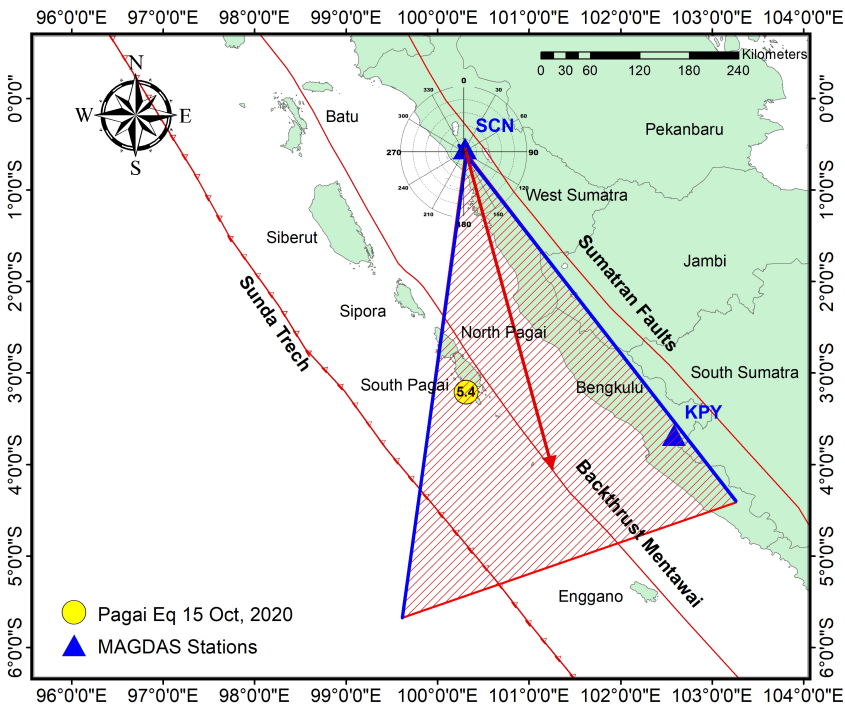


Fig. 3. ULF anomaly azimuth (red arrow) from SCN station (blue triangle) to the earthquake of October 15, 2020 ($M_w = 5.4$) (yellow circle) with an azimuth tolerance of 22.5° (blue line).

tolerance area for the estimated azimuth of the anomaly of October 3, 2020 from the SCN station. The azimuth of other ULF anomalies did not point to the source area of the 15 October 2020 earthquake.

In a similar way, azimuth direction of the ULF emission anomaly concerning to the earthquake precursors of 17 October 2020 ($M_W = 5.2$), 18 October 2020 ($M_W = 5.3$), 19 October 2020 ($M_W = 5.1$), 21 October 2020 ($M_W = 5.1$), and 17 November 2020 ($M_W = 5.9$) were also determined. A list of azimuths for all anomalies can be seen in Tables 4 and 5. Overall, Table 6 shows the onset time of anomalies indicated as precursors of all earthquakes studied. The azimuth generated by the ULF emission anomaly still included the azimuth of the earthquake being studied, where the azimuth generated from the anomaly (θ_A) had a value not much different from the actual earthquake azimuth (θ_{EQ}) to the observation station. Thus, the earthquake location estimation based on the overall azimuth direction for the Pagai Island area was very effective to be used with an accuracy of 97.08%. This accuracy was derived from $\Delta\theta_{\%}$ based on the following equation (Yusof *et al.*, 2021):

$$\theta\Delta = \theta_{EQ} - \theta, \quad (14)$$

$$\theta\Delta_{\%} = \frac{|\Delta\theta|}{360^{\circ}} \times 100\%, \quad (15)$$

where θ_{EQ} is the actual earthquake azimuth to the station, θ is the ULF anomaly azimuth, $\Delta\theta$ is the difference (error) degree between the earthquake azimuth and anomaly azimuth ($^{\circ}$), and $\Delta\theta_{\%}$ is the percentage difference (error) between the earthquake azimuth and the anomaly azimuth.

However, this azimuth-based analysis still allowed for some biases because the earthquakes of October 17, 2020 ($M_W = 5.2$), October 18, 2020 ($M_W = 5.3$), October 19, 2020 ($M_W = 5.1$), and October 21, 2020 ($M_W = 5.1$) occurred with time and a location close to October 15, 2020 ($M_W = 5.4$) (Fig. 1). Thus, the anomaly on October 3, 2020 (06:00 LT) which was probably caused by the earthquake preparation zone on October 15, 2020 ($M_W = 5.4$), could not be used yet as a precursor for the earthquake of October 15, 2020 ($M_W = 5.4$) because other earthquakes also occurred at a time and location close to this earthquake. To prevent any bias of analysis on the anomaly source based on this azimuth, an estimation of the earthquake magnitude was carried out as described in the following sub-chapter.

Table 6. Comparison between the estimated earthquake azimuth of the onset time of ULF anomaly value and the actual earthquake azimuth.

No.	Date of EQ ¹	Time ² [LT]	Sta ³ [code]	Date of An ⁴	Time ⁵ [LT]	θ_A ⁶ [°]	θ_{EQ} ⁷ [°]	$\Delta\theta$ ⁸ [°]	Dst ⁹ [nT]
1	October 15, 2020	16:41:16	SCN	October 3, 2020	06:00:00	165	178	13	-27
2	October 17, 2020	07:26:02	KPY	October 4, 2020	17:00:00	272	282	10	-11
3	October 18, 2020	00:55:00	KPY	October 15, 2020	03:00:00	292	277	4	-3
4	October 19, 2020	05:48:50	KPY	October 15, 2020	20:00:00	266	276	-15	-1
5	October 21, 2020	21:35:09	KPY	October 17, 2020	18:00:00	265	278	13	-5
6	November 17, 2020	08:44:07	KPY	October 17, 2020	08:00:00	281	279	-2	-2

¹ Date of earthquake, ² occurrence time of earthquake in local time [LT], ³ nearest observation station to the earthquake source (code), ⁴ date of ULF anomaly as earthquake precursor, ⁵ occurrence time of anomaly in local time [LT], ⁶ anomaly azimuth from observation station, ⁷ actual earthquake azimuth to observation station, ⁸ difference of anomaly azimuth to earthquake azimuth, ⁹ Dst index.

3.3. Estimation of earthquake magnitude

Table 7 presents the estimated magnitude values for all earthquakes. The earthquake magnitude was estimated by empirical formula of *BMKG (2019)* with a tolerance value of ± 0.2 . The results of the magnitude estimation of the October 15, 2020 earthquake using the ULF emission anomaly of October 3, 2020 (06:00 LT) showed the anomaly amplitude value of 2.07. This amplitude was used to estimate the earthquake magnitude that will occur. The estimated magnitude of the October 15, 2020 earthquake was 5.2 or with a magnitude value range of 5.0–5.4 (± 0.2). This estimated value was close to the actual magnitude of the October 15, 2020 earthquake, i.e. 5.4.

Overall, the earthquake magnitude estimated from the onset time ULF anomaly value was within the tolerance range for the estimated magnitude; thus, the anomaly can be considered as the earthquake precursor (Table 7). The magnitude of earthquake based on ULF anomaly had an accuracy of 98.13% compared to magnitude of earthquake occurred, where the differ-

Table 7. Comparison between the estimated earthquake magnitude from the onset time of ULF anomaly value and the actual earthquake magnitude.

No.	Date of EQ ¹	Time ² [LT]	Date of An ³	Time ⁴ [LT]	Sta ⁵ [code]	A ⁶	MA ⁷ [± 0.2]	MEQ ⁸ [M_W]	ΔM ⁹	τ ¹⁰ [day]
1	October 15, 2020	16:41:16	October 3, 2020	06:00:00	SCN	2.07	5.2	5.4	-0.2	12
2	October 17, 2020	07:26:02	October 4, 2020	17:00:00	KPY	5.06	5.2	5.2	0.0	13
3	October 18, 2020	00:55:00	October 15, 2020	03:00:00	KPY	2.25	5.2	5.3	-0.1	3
4	October 19, 2020	05:48:50	October 15, 2020	20:00:00	KPY	2.24	5.2	5.1	+0.1	4
5	October 21, 2020	21:35:09	October 17, 2020	18:00:00	KPY	4.25	5.2	5.1	-0.1	4
6	November 17, 2020	08:44:07	October 17, 2020	08:00:00	KPY	27.95	5.8	5.9	-0.1	31

¹ Date of earthquake, ² occurrence time of earthquake in local time [LT], ³ date of anomaly as earthquake precursor, ⁴ occurrence time of anomaly in local time [LT], ⁵ nearest observation station to the earthquake source (code), ⁶ ULF anomaly amplitude, ⁷ estimated earthquake magnitude based on ULF anomaly, ⁸ real magnitude of earthquake, ⁹ magnitude difference between estimated and actual earthquake magnitude, ¹⁰ lead times of anomaly.

ence in the magnitude of the earthquake that occurs is still in the estimated magnitude value. The earthquake that has the closest magnitude to the estimated magnitude is the October 17, 2020 earthquake. This earthquake has an anomaly onset time amplitude of ULF 5.06 (A) and the estimated magnitude of the earthquake is 5.2 [± 0.2]. This estimated magnitude value is the same as the magnitude of the 17 October 2020 earthquake is 5.2. The other earthquakes have a fairly small difference in the estimated magnitude of the earthquake that has occurred is ± 0.1 . This showed that earthquakes with a magnitude < 6 can be estimated very well using the anomalous amplitude.

The lead time of precursor is important for short-term earthquake prediction. We calculated the lead time by first determining the onset time based on the time the anomaly first appeared as a precursor. For example, the onset time of the ULF emission anomaly for the 15 October 2020 earthquake ($M_W = 5.4$) was 3 October 2020. The lead time (τ) of the 15 October 2020 earthquake precursor ($M_W = 5.4$) was the day calculated

from the time the anomaly first appeared (3 October 2020) until the time of earthquake occurred (15 October 2020). Thus, the lead time of ULF emission anomaly for the 15 October 2020 earthquake is 12 days. A list of anomaly lead time for all earthquakes can be seen in Table 7. The ULF anomaly as the earthquake precursor on Pagai Island occurred 3–13 days before the earthquake, except for the November 17, 2020 earthquake. This result is consistent with *Ibrahim et al. (2012)* and *Ahadi et al. (2015)* who found the onset time of ULF anomaly 3–11 days.

4. Conclusions

This study showed the effectiveness of determining ULF anomalies as earthquake precursors in Pagai Island by using earthquake magnitude estimates based on the occurred anomalies. The estimated azimuth obtained from this study had an accuracy value of 97.08% compared to the actual azimuth of the earthquake. Furthermore, the estimated magnitude had an accuracy of 98.13% of the earthquake's magnitude. The azimuth and magnitude estimation techniques are effective in determining precursors for earthquakes with adjacent time and source locations. The results of this study can be a solution for any bias possibility in determining earthquake precursors for such earthquakes, particularly in areas with high earthquake frequencies.

Funding. The present study was supported by 2021 Research Grants for Publication to Support the Professor Acceleration Programme from Universitas Andalas (PDU-KRP2GB-UNAND)(contract No. T/11/UN.16.17/PP.IS-PDU-KRP2GB-Unand/LPPM/2021).

Data availability statement. Publicly available datasets were analysed in this study. The earthquakes data can be found here: <http://repogempa.bmkg.go.id>, and Disturbance storm time index can be found here: <http://wdc.kugi.kyoto-u.ac.jp>. The magnetic data was obtained from Meteorology Climatology and Geophysical Agency (BMKG) and are available from Suadi Ahadi with the permission of BMKG.

Acknowledgements. Thanks to the Meteorology Climatology and Geophysical Agency (BMKG) for providing geomagnetic data of earthquake and WDC Geomagnetic Models, Kyoto University for providing Disturbance storm time index data, and Universitas Andalas for funding this research. We also acknowledge the assistance of Ravidho Ramadhan and Helmi Yusnaini in plotting some data.

References

- Ahadi S., 2014: Analysis of precursor patterns for the 2007–2012 strong Sumatran earthquakes based on ULF emissions (Ultra-Low-Frequency) using geomagnetic data (Analisis pola prekursor gempa bumi kuat Sumatera periode 2007–2012 berdasarkan emisi ULF (Ultra-Low-Frequency) menggunakan data geomagnet). Ph.D. Thesis, Institut Teknologi Bandung, Bandung (in Indonesian with English summary).
- Ahadi S., Puspito N. T., Ibrahim G., Saroso S., 2014: Determination of the onset time in polarization power ratio Z/H for precursor of Sumatera earthquake. AIP Conference Proceedings 1617, 75, 3rd International Conference on Theoretical and Applied Physics., doi: 10.1063/1.4897108.
- Ahadi S., Puspito N. T., Ibrahim G., Saroso S., Yumoto K., Yoshikawa A., Muzli L., 2015: Anomalous ULF emissions and their possible association with the strong earthquakes in Sumatra, Indonesia, during 2007–2012. J. Math. Fundam. Sci., 47, 1, 84–103, doi: 10.5614/j.math.fund.sci.2015.47.1.7.
- Armansyah, Fatimah A., Ahadi S., 2016: Study of ultra-low frequency Earth magnetic signal anomaly as earthquake precursor for small magnitude earthquake events (Studi Anomali Sinyal Magnet Bumi Ultra Low Frequency Sebagai Prekursor Gempa Bumi Untuk Kasus Kejadian Gempa Bumi Dengan Magnitudo Kecil). Seminar Nasional Fisika dan Aplikasinya Preceeding, ISSN: 2447-0477 (in Indonesian with English summary).
- BMKG (Meteorology Climatology and Geophysical Agency), 2019: Earthquake precursor kaleidoscope using Earth magnet data for Sumatra region 2016–2018 (Kaleidoskop Prekursor Gempa Bumi dengan Menggunakan Data Magnet Bumi Wilayah Sumatera Tahun 2016–2018). Jakarta, Indonesia.
- Han P., Hattori K., Huang Q., Hirano T., Ishiguro Y., Yoshino C., Febriani F., 2011: Evaluation of ULF electromagnetic phenomena associated with the 2000 Izu Islands earthquake swarm by wavelet transform analysis. Nat. Hazards Earth Syst. Sci., 11, 3, 965–970, doi: 10.5194/nhess-11-965-2011.
- Hattori K., 2004: ULF Geomagnetic Changes Associated with Large Earthquakes. Terr. Atmos. Ocean. Sci., 15, 3, 329–360. doi: 10.3319/TA0.2004.15.3.329(EP).
- Hattori K., Akinaga Y., Hayakawa M., Yumoto K., Nagao T., Uyeda S., 2002a: ULF magnetic anomaly preceding the 1997 Kagoshima earthquakes. In: Hayakawa M., Molchanov O. A. (Eds.): Seismo Electromagnetics: Lithosphere–Atmosphere–Ionosphere Coupling. Terra Scientific Publishing Company: Tokyo, Japan., 19–28.
- Hattori K., Takahashi I., Yoshino C., Nagao T., Liu J. Y., Shieh C. F., 2002b: ULF Geomagnetic and Geopotential Measurement at Chia-Yi, Taiwan. J. Atmos. Electr., 22, 3, 217–222, doi: 10.1541/jae.22.217.
- Hattori K., Han P., Huang Q., 2011: Global variation of ULF geomagnetic fields and detection of anomalous changes at a certain observatory using reference data. IEEEJ Trans. Fundam. Mater., 131, 9, 698–704, doi: 10.1541/ieejfms.131.698.
- Hattori K., Han P., Yoshino C., Febriani F., Yamaguchi H., Chen C.-H., 2013: Investigation of ULF seismo-magnetic phenomena in Kanto, Japan during 2000–2010: Case studies and statistical studies. Surv. Geophys., 34, 3, 293–316, doi: 10.1007/s10

712–012–9215–x.

- Ibrahim G., Ahadi S., Saroso S., 2012: Characteristic ulf emissions possibly associated with earthquake precursor in Sumatra, case study: Padang earthquake 2009, and Mentawai earthquake 2010 (Karakteristik sinyal emisi ULF yang berhubungan dengan prekursor gempa bumi di Sumatera, studi kasus: gempa bumi Padang 2009 dan gempa bumi Mentawai 2010). *Jurnal Meteorologi dan Geofisika*, **13**, 2, 81–89, doi: 10.31172/jmg.v13i2.122 (in Indonesian with English summary).
- Loewe C. A., Prölss G. W., 1997: Classification and mean behavior of magnetic storms. *J. Geophys. Res. Space Phys.*, **102**, 14209–14213, doi: 10.1029/96JA04020.
- Mogi K., 1985: Earthquake Prediction. Academic press, Tokyo, Japan.
- Molchanov O. A., Hayakawa M., 1995: Generation of ULF electromagnetic emissions by microfracturing. *Geophys. Res. Lett.*, **22**, 22, 3091–3094, doi: 10.1029/95GL00781.
- Molchanov O. A., Hayakawa M., 1998: On the generation mechanism of ULF seismogenic electromagnetic emissions. *Phys. Earth Planet. Inter.*, **105**, 3–4, 201–210, doi: 10.1016/S0031-9201(97)00091-5.
- Molchanov O. A., Schekotov A., Fedorov E., Belyav G., Gordeev E., 2003: Preseismic ULF electromagnetic effect from observation at Kamchatka. *Nat. Hazards Earth Syst. Sci.*, **3**, 3–4, 203 – 209, doi: 10.5194/nhess-3-203-2003.
- Parkinson W. D., 1959: Directions of rapid geomagnetic fluctuations. *Geophys. J. Int.*, **2**, 1, 1–14, doi: 10.1111/j.1365-246X.1959.tb05776.x.
- Prattes G., Schwingenschuh K., Eichelberger H. U., Magnes W., Boudjada M., Stachel M., Vellante M., Villante U., Wesztergom V., Nenovski P., 2011: Ultra Low Frequency (ULF) European multi station magnetic field analysis before and during the 2009 earthquake at L’Aquila regarding regional geotechnical information. *Nat. Hazards Earth Syst. Sci.*, **11**, 7, 1959–1968, doi: 10.5194/nhess-11-1959-2011.
- Purba S. F., Nuraeni F., Utama J. A., 2013: Application of ULF signal polarization method in solar activity influence separation from geomagnet anomaly related to earthquake (Penerapan metode polarisasi sinyal ULF dalam pemisahan pengaruh aktivitas matahari dari anomali geomagnet terkait gempa bumi). *Fibusi (Jurnal Online Fisika)*, **1**, 3, 1–5 (in Indonesian with English summary).
- Rikitake T., Honkura Y., 1985: Solid Earth Geomagnetism, 1st edition. Terra Scientific Publishing Company: Tokyo, Japan.
- Saroso S., Hattori K., Ishikawa H., Ida Y., Shirogane R., Hayakawa M., Yumoto K., Shiokawa K., Nishihashi M., 2009: ULF geomagnetic anomalous changes possibly associated with 2004–2005 Sumatra earthquake. *Phys. Chem. Earth*, **34**, 6–7, 343–349, doi: 10.1016/j.pce.2008.10.065.
- Scordilis E. M., 2006: Empirical global relations converting M_S and m_b to moment magnitude. *J. Seismol.*, **10**, 225–236, doi: 10.1007/s10950-006-9012-4.
- Uozumi T., Yumoto K., Kitamura K., Abe S., Kakinami Y., Shinohara M., Yoshikawa A., Kawano H., Ueno T., Tokugana T., McNamara D., Ishituka J. K., Dutra S. L. G., Damtie B., Doumbia V., Obrou O., Rabui A. B., Adimula I. A., Othman M., Fairoos M., Otadoy R. E. S., MAGDAS Group, 2008: A new index to monitor temporal and long-term variations of the equatorial electrojet by MAGDAS/CPMN real-time data: *EE-Index*. *Earth Planets Space*, **60**, 7, 785–790, doi: 10.1186/BF03352828.

- Yumoto K., Ikemoto S., Cardinal M. G., Hayakawa M., Hattori K., Liu J. Y., Saroso S., Ruhimat M., Husni M., Widarto D., Ramos E., McNamara D., Otadoy R. E. S., Yumul G., Eborá R., Servando N., 2009: A new ULF wave analysis for Seismo-Electromagnetics using CPMN/MAGDAS data. *Phys. Chem. Earth*, **34**, 6-7, 360–366, doi: 10.1016/j.pce.2008.04.005.
- Yusof K. A., Abdulla M., Hamid N. S. A., Ahadi S., Yoshikawa A., 2021: Correlation between earthquake properties and characteristics of possible ULF geomagnetic precursor over multiple earthquake. *Universe*, **7**, 1, 1–17, doi: 10.3390/universe7010020.